

Critical Currents of Josephson-Coupled Wire Arrays

J. Kent Harbaugh and D. Stroud
 (February 1, 2008)

We calculate the current-voltage characteristics and critical current I_c^{array} of an array of Josephson-coupled superconducting wires. The array has two layers, each consisting of a set of parallel wires, arranged at right angles, such that an overdamped resistively-shunted junction forms wherever two wires cross. A uniform magnetic field equal to f flux quanta per plaquette is applied perpendicular to the layers. If $f = p/q$, where p and q are mutually prime integers, $I_c^{\text{array}}(f)$ is found to have sharp peaks when q is a small integer. To an excellent approximation, it is found in a square array of n^2 plaquettes, that $I_c^{\text{array}}(f) \propto (n/q)^{1/2}$ for sufficiently large n . This result is interpreted in terms of the commensurability between the array and the assumed $q \times q$ unit cell of the ground state vortex lattice.

I. INTRODUCTION

There has been much recent interest in Josephson junction arrays with so-called long-range interactions. Such arrays typically consist of two layers of N parallel superconducting wires, arranged at right angles, in such a fashion that a Josephson junction is formed at each point where two wires cross (see Fig. 1). In this geometry, each wire in one layer is Josephson-coupled to all the wires in the other layer. If $N \gg 1$, each wire has many “nearest-neighbor” wires to which it is coupled. Under these conditions, the thermodynamic properties of the array are accurately described by mean-field theory. Indeed, it has been shown¹ that the usual mean-field theory for phase transitions in such arrays in a transverse magnetic field² becomes exact in the limit $N \rightarrow \infty$, provided that each wire can be considered as a locus of constant superconducting phase. Experiments on finite arrays ($N \approx 17$) have recently confirmed the accuracy of mean-field predictions.³ For very large arrays, the assumption that each wire is a locus of constant phase breaks down, and the mean-field theory has to be corrected to take account of the phase variation along the array.⁴ This same effect causes the critical current of the array to saturate at a finite value which depends on the Josephson penetration depth, even as $N \rightarrow \infty$.^{5,6}

The exactness of mean-field theory is believed to have an analog in the *dynamics* of these arrays. Chandra *et al.*^{7,8} have studied a version of local dynamics equivalent, in the large- N limit, to the resistively-shunted junction (RSJ) model with Gaussian thermal noise and no applied current (they use a different numerical approach from that followed here). In the dynamical case, the effects of magnetic-field-induced frustration combine with those arising from the fact that each wire has many other “nearest-neighbor” wires with which it interacts. The result is a kind of glassy behavior, with many metastable states separated by large energy barriers, critical slowing down near the phase transition, and typically glassy aging effects.

In this paper, we extend the RSJ model described above to include applied currents. Specifically, we calculate the current-voltage (*IV*) characteristics and the critical currents I_c^{array} for arrays of crossed Josephson junctions, in typical experimental geometries as shown in Fig. 1. We assume that, even though $N \gg 1$, each wire can be taken as a locus of constant phase, and we study how I_c^{array} is affected by a transverse magnetic field of magnitude f flux quanta per plaquette. Our principal result is that $I_c^{\text{array}}(f)$ is extremely sensitive to f , in a manner related to the commensurability between the lattice and the vortex structure of the induced array supercurrents. A similar sensitivity is found in the array critical temperature $T_c(f)$, as calculated by mean-field theory,⁵ and as confirmed in detail by experiments. It would be of great interest if similar experiments could be carried out to confirm our calculated $I_c^{\text{array}}(f)$.

We turn now to the body of the paper. In Section II we describe the geometry of our calculations and the model used to calculate the *IV* characteristics and I_c^{array} . Our numerical results are given in Section III, followed by a brief discussion in Section IV.

II. MODEL

As shown in Fig. 1, the array consists of two layers of parallel superconducting wires arranged at right angles. A resistively shunted Josephson junction is assumed to form at each point where two wires cross. To determine I_c^{array} , we assume that a constant bias current I_B is injected into one wire and extracted from a different wire. The *IV* characteristics are determined by calculating the time-averaged voltage drop across these two wires. We consider two configurations for current injection. In the first, the current is injected into a wire at the left edge of one layer and extracted from the wire at the right edge of the same layer (left-hand side of Fig. 1). In the other configuration, the input and output wires are centered in different layers of the array (cf. right-hand side of Fig. 1). We also assume that a time-independent, uniform magnetic field B is applied perpendicular to the array, of magnitude $B = f\Phi_0/a^2$, where $\Phi_0 = hc/(2e)$ is the flux quantum, and a^2 is the area of each square plaquette.

We assume that the phase of the superconducting order parameter is a constant on each wire, independent of position along the wire.⁹ With this assumption, we can write down the equations determining the flow of current through the system. We assume an array of $N \times M$ wires, and model the intersections between the crossed wires as overdamped, resistively-shunted Josephson junctions. The equations determining the time-variation of phases on each wire can then be written down using Kirchhoff’s Laws. For example, in the perpendicular current input configuration, the equations take the form

$$I_B \delta_{jm} = \sum_{k=1}^N [I_c \sin(\psi_j - \phi_k - A_{kj}) + I_{kj} + I_{L;kj}],$$

$$I_B \delta_{kn} = \sum_{j=1}^M [I_c \sin(\psi_j - \phi_k - A_{kj}) + I_{kj} + I_{L;kj}]. \quad (1)$$

Here I_B is the constant bias current, which is injected into wire m in one layer and extracted from wire n in the other layer; ϕ_k is the phase of the k th wire in one layer; and ψ_j is that of the j th wire in the other layer. I_c denotes the critical current of a junction formed at the intersection of any two wires (the junctions are assumed to be identical). The supercurrent flowing through the ij th junction is then $I_c \sin(\psi_j - \phi_k - A_{kj})$, where the quantity in parentheses is the gauge-invariant phase difference across the junction. We use a gauge such that the phase factor A_{kj} arising from the vector potential of the magnetic field is $A_{kj} = 2\pi k j B a^2 / \Phi_0$.¹⁰ I_{kj} denotes the normal current through the shunt resistance R in the junction at coordinates (ka, ja) ; it is given by

$$I_{kj} = \frac{\hbar}{2eR} \frac{d}{dt} (\psi_j - \phi_k - A_{kj}). \quad (2)$$

Finally, at finite temperatures, one must also include a Langevin noise current $I_{L;kj}$ in parallel to the other currents. In the present calculations, we assume temperature $T = 0$, so that $I_{L;kj}$ vanishes.¹¹ The equations describing the parallel current injection can be written down in an analogous fashion.

Eqs. (1) can be conveniently expressed in a dimensionless form, such that current is measured in units of I_c , and time in units of $\hbar/(2eI_c R)$, and then rewritten in a fashion which is more convenient for numerical solution. First, we rearrange Eqs. (1) to obtain

$$\dot{\phi}_k = \frac{1}{N} \sum_{i=1}^N \dot{\phi}_i + \frac{1}{NM} \left[i_B - \sum_{i=1}^N \sum_{j=1}^M \sin(\psi_j - \phi_i - A_{ij}) \right]$$

$$- \frac{1}{M} \left[i_B \delta_{kn} - \sum_{j=1}^M \sin(\psi_j - \phi_k - A_{kj}) \right],$$

$$\dot{\psi}_k = \frac{1}{N} \sum_{i=1}^N \dot{\phi}_i + \frac{1}{N} \left[i_B \delta_{km} - \sum_{i=1}^N \sin(\psi_k - \phi_i - A_{ik}) \right]. \quad (3)$$

Of the $N+M$ degrees of freedom in these equations, one may be chosen freely. We fix this degree of freedom by arbitrarily choosing

$$\frac{1}{N} \sum_{i=1}^N \dot{\phi}_i = -\frac{1}{2NM} \left[i_B - \sum_{i=1}^N \sum_{j=1}^M [\sin(\psi_j - \phi_i - A_{ij})] \right]. \quad (4)$$

With this choice, and making use of the double-angle formulas for the sines and cosines, Eqs. (3) take the final form

$$-\dot{\phi}_k = -\frac{1}{2NM} \left[i_B - \sum_{i=1}^N \sum_{j=1}^M \sin(\psi_j - \phi_i - A_{ij}) \right]$$

$$+ \frac{1}{M} \left[i_B \delta_{kn} - \sum_{j=1}^M \sin(\psi_j - \phi_k - A_{kj}) \right],$$

$$\dot{\psi}_k = -\frac{1}{2NM} \left[i_B - \sum_{i=1}^N \sum_{j=1}^M \sin(\psi_j - \phi_i - A_{ij}) \right]$$

$$+ \frac{1}{N} \left[i_B \delta_{km} - \sum_{i=1}^N \sin(\psi_k - \phi_i - A_{ik}) \right]. \quad (5)$$

The form of these equations is quite suggestive. Namely, the time-variation of phases in *one* layer depends only on certain averages over phases in the *other* layer. A similar result is known to hold for the averages of certain *equilibrium* functions of the phases in each layer, in the thermodynamic (i.e. large N and large M) limits. A consequence of this result in the equilibrium case is that mean-field theory is exactly valid for the thermodynamics of this system in the limit of large N and large M .¹

Although we have not found an analytical solution to these dynamical equations, they are easily solved numerically for any N and M using a standard Runge-Kutta method. We have used a fixed-step-size, fourth-order Runge-Kutta algorithm, with time steps ranging between 0.01 and 0.1 dimensionless time units. We obtained the d.c. voltage V by averaging the instantaneous voltage over 100 time units. In order to obtain the IV characteristics, the input current was slowly swept from high to low currents.¹² After each current step, the system was given 100 time units to reach steady state before the time-averaged voltage was computed. Zero-temperature calculations were carried out for two different $N \times N$ array sizes, $N = 18$ and $N = 14$, for each input configuration.

III. RESULTS

Figure 2 shows the calculated IV curves for several fields in the *parallel* current configuration. The field is expressed in terms of the *frustration* $f = Ba^2/\Phi_0$, the number of flux quanta per plaquette. By definition, the array critical current I_c^{array} is the largest bias current for which the time-averaged voltage $\langle V \rangle_t = 0$. By inspection of Fig. 2, I_c^{array} is considerably suppressed by application of a finite magnetic field. If f is a rational fraction denoted $f = p/q$ where p and q are integers with no common factors, then the figure also shows that $I_c^{\text{array}}(f)$ is suppressed more at frustrations with larger values of q .

These observations are made more quantitative in Figs. 3 and 4, which show the calculated $I_c^{\text{array}}(f)$ for a wide range of fields. Figure 3 shows $I_c^{\text{array}}(f)$ for an 18×18 array in both the perpendicular (top) and parallel (bottom) input current configurations. In this case, $I_c^{\text{array}}(f)$ was obtained by directly calculating the voltage across the array for a range of bias currents and recording the highest current with a zero mean voltage. In order to reduce the numerical noise, we have smoothed the critical current data as a function of frustration with a Savitzky-Golay filter.¹³ Clearly, $I_c^{\text{array}}(f)$ has sharp peaks near fractions $f = p/q$ with small denominators q .

Since it can be difficult to determine numerically the precise current at which $\langle V \rangle_t \rightarrow 0$, we have also calculated $I_c^{\text{array}}(f)$ by extrapolating the IV curve above I_c^{array} , assuming the functional form

$$\left[\frac{V}{I_c R} \right]^2 = m^2 \left[\left(\frac{I_B}{I_c} \right)^2 - \left(\frac{I_c^{\text{array}}}{I_c} \right)^2 \right], \quad (6)$$

and determining m and I_c^{array} by the least-squares fitting procedure. The resulting data were also smoothed using the same Savitzky-Golay filter. This extrapolation algorithm, used to calculate the data in Fig. 4, considerably reduces the numerical noise near I_c^{array} , and the smaller peaks in $I_c^{\text{array}}(f)$ stand out more clearly than in the direct calculation. Using this procedure, we have calculated $I_c^{\text{array}}(f)$ for both an 18×18 (top) and a 14×14 (bottom) array in the *parallel* current injection configuration. Clearly, there are peaks in $I_c^{\text{array}}(f)$ at all fractions $f = p/q$ such that $q \leq 16$ in the larger array or $q \leq 12$ in the smaller array. We now discuss some possible reasons for this behavior.

IV. DISCUSSION

The present results show that $I_c^{\text{array}}(f)$ is a sensitive function of the applied field f . At $f = 0$, the array is unfrustrated and $I_c^{\text{array}}(f)$ is maximized. At a rational frustration $f = p/q$ where p and q are integers with no common factor and $q \leq N - 2$, our numerical results suggest that height of the peaks in $I_c^{\text{array}}(f)$ approximately obeys the relation

$$i_c^{\text{array}} \sim r^{1/4} (s/P^2)^{1/2}. \quad (7)$$

Here r is the number of flux lattice unit cells (assumed to be of size $q \times q$) which can be inscribed in the array, $s = rq^2$ is the number of array plaquettes which are contained in all r of the $q \times q$ cells, and $P^2 = (N - 1)^2$ is the total number of plaquettes in the array ($N = M$ in a square array). This form can be made explicit by writing $r = (\text{int}[P/q])^2$, where $\text{int}[x]$ is the greatest integer $n \leq x$. Then Eq. 7 can also be written as

$$i_c^{\text{array}} \sim (q/P)(\text{int}[P/q])^{3/2}. \quad (8)$$

In the limit of large N , this result takes the even simpler form

$$i_c^{\text{array}} \sim (n/q)^{1/2}, \quad (9)$$

where $n = N - 1$. The values predicted by eq. 7 are plotted as crosses in Fig. 4. Agreement with the numerical data is remarkably good.

We can understand Eq. 7 as a measure of the commensurability between the field and the array. We expect that, just as in more conventional Josephson arrays with square plaquettes, the ground state energy configuration in a field $f = p/q$ and no applied current has a flux lattice unit cell consisting of $q \times q$ plaquettes. A *finite* wire array at a given field can contain a certain number of such cells, with a number of plaquettes left over. We may expect that the current required to depin such unit cells, and hence $I_c^{\text{array}}(f)$, will increase as the number of flux lattice unit cells which can fit into the array becomes larger, and the number of “remainder” plaquettes becomes smaller. Indeed our analytical expression, which fits our numerical data, expresses $I_c^{\text{array}}(f)$ in this fashion. Note also that, according to Eq. 9, for large values of N , $i_c^{\text{array}} \sim q^{-1/2}$. Thus, in this regime, $i_c^{\text{array}}(f)$ depends on q in the same way as the mean-field transition $T_c(f)$ reported

in Ref.³. The proportionality between $i_c^{\text{array}}(f)$ and $T_c(f)$ is the same as that which is believed to hold between critical current and transition temperature in more conventional two-dimensional Josephson junction arrays.¹⁴

Finally, we comment briefly on our results in light of the work of Refs.^{7,8}. Their picture of frustrated arrays may well hold true even in the presence of an applied current. However, it is difficult to draw any quantitative conclusions from our own calculations about the energy barriers they discuss, other than those which are suggested by the field-dependence of the critical current. These results obviously suggest that the barriers are smallest for largest values of q , though the reasons for the analytical dependence ($\propto q^{-1/2}$) remain a matter for speculation.

V. ACKNOWLEDGMENTS

We gratefully acknowledge support by the National Science Foundation, through grant DMR97-31511.

¹ V. M. Vinokur, L. B. Ioffe, A. I. Larkin, and M. V. Feigelman, Zh. Eksp. Teor. Fys. **93**, 343 (1987) [Sov. Phys. JETP **66**, 198 (1987)].

² W. Y. Shih and D. Stroud, Phys. Rev. B **28**, 6575 (1983).

³ L. L. Sohn, M. T. Tuominen, M. S. Rzchowski, J. U. Free, and M. Tinkham, Phys. Rev. B **47**, 975 (1993); L. L. Sohn, M. S. Rzchowski, J. U. Free, and M. Tinkham, Phys. Rev. B **47**, 967 (1993).

⁴ J. Kent Harbaugh and D. Stroud, Phys. Rev. B **56**, 8335 (1997).

⁵ H. R. Shea and M. Tinkham, Phys. Rev. Lett. **79**, 2324 (1997).

⁶ J. Kent Harbaugh and D. Stroud, Phys. Rev. B (in press)

⁷ P. Chandra, M. V. Feigelman, and L. B. Ioffe, Phys. Rev. Lett. **76**, 4805 (1996).

⁸ P. Chandra, M. V. Feigelman, and L. B. Ioffe, Phys. Rev. B **56**, 11553 (1997).

⁹ In order for this condition to prevail, the array size must be less than the Josephson screening length,⁶ i.e., for a square array, $N \ll \sqrt{I_c^{\text{wire}}/I_c}$. Of course, even if this condition holds, the phase is constant along the wire only if a particular gauge is chosen, as discussed below.

¹⁰ We choose a gauge such that the phase variables are constant on each wire and the dependence on applied magnetic field is contained entirely in the factors A_{kj} , as shown in Eq. (1). See Ref.⁶ for a discussion of this gauge in a slightly different context.

¹¹ The method is described in more generality in, for example, J. S. Chung, K. H. Lee, and D. Stroud, Phys. Rev. B **40**, 6570 (1989).

¹² The calculated *IV* curves appeared to be non-hysteretic, except for small, apparently random fluctuations near I_c^{array} .

¹³ Specifically, we replaced each unfiltered data point by a Savitzky-Golay fourth-order weighted mean over the five unfiltered data points on either side of that data point [see, e.g., W. H. Press, S. A. Teukolsky, W. T. Vetterling, and B. P. Flannery, *Numerical Recipes*, 2nd Ed., Cambridge Univ. Press, 1992, §14.8].

¹⁴ S. Teitel and C. Jayaprakash, Phys. Rev. Lett. **50**, 1999 (1983).

FIG. 1. Sketch of array geometry. The array consists of two layers of parallel wires, arranged at right angles. A resistively-shunted Josephson junction forms at each wire intersection. There are two configurations for the current injection: *parallel* injection and extraction wires (shown on left); and *perpendicular* injection and extraction wires (on right).

FIG. 2. Current-voltage curves at several frustrations for an 18×18 array with *parallel* input wire configuration. V denotes time-averaged voltage between input and output wires.

FIG. 3. The critical current $I_c^{\text{array}}(f)$ plotted versus frustration f for an 18×18 array in the *perpendicular* input wire configuration (upper plot) and the *parallel* configuration (lower plot). These data are obtained from a direct calculation, smoothed using the Savitzky-Golay filter.¹³ The hash marks at top denote each rational frustration $f = p/q$ with $q \leq 16$. Frustrations with $p = 1$ are denoted with bold hash marks.

FIG. 4. $I_c^{\text{array}}(f)$ for an 18×18 array (upper plot) and a 14×14 array (lower plot) in the *parallel* input wire configuration. These data are calculated by a least-squares fit to the functional form of Eq. 6, then smoothed using the Savitzky-Golay filter.¹³ Hash marks at top denote each rational frustration $f = p/q$ with $q \leq 16$ (upper plot) or $q \leq 12$ (lower plot). Frustrations with $p = 1$ have bold hash marks. The \times symbols denote the peak heights as predicted by Eq. 8, using the same, arbitrary normalization for each plot.

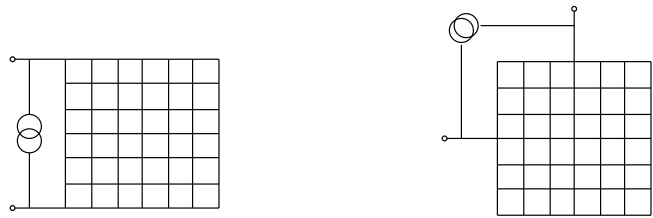


FIG. 1. Critical Currents of Josephson-Coupled Wire Arrays. J. Kent Harbaugh and D. Stroud.

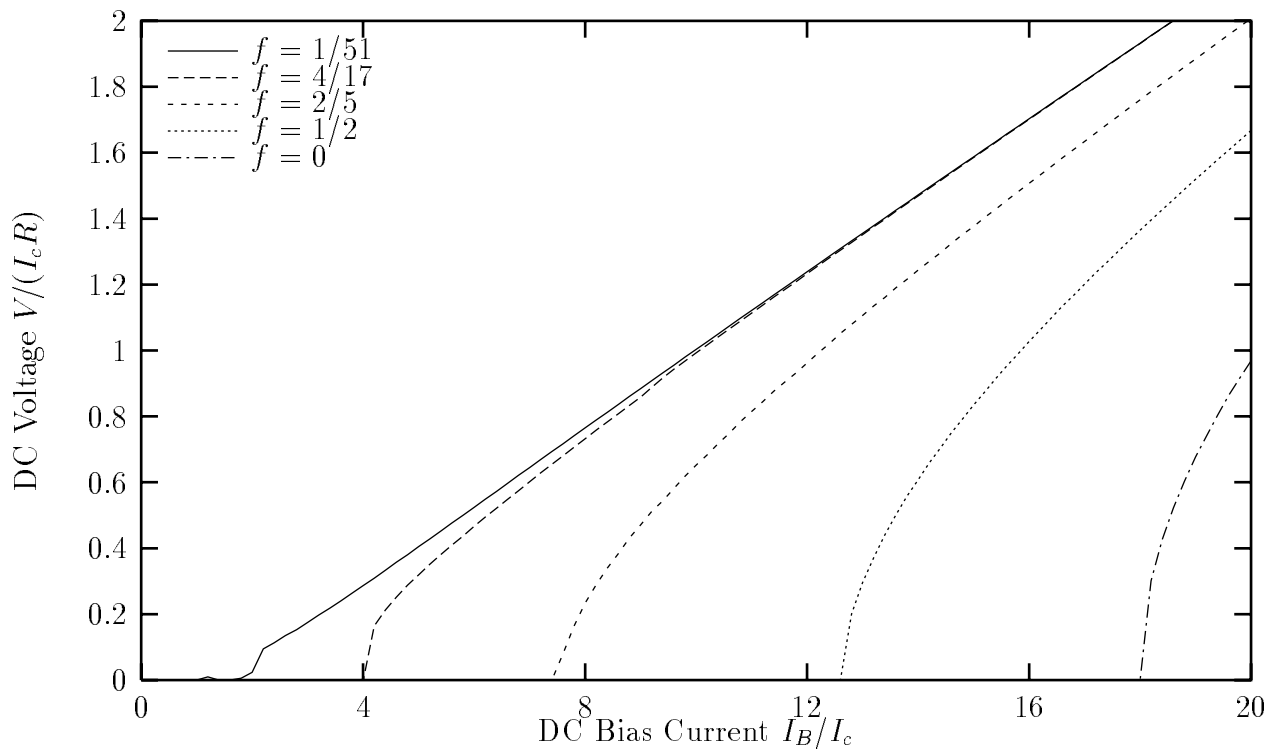


FIG. 2. Critical Currents of Josephson-Coupled Wire Arrays. J. Kent Harbaugh and D. Stroud.

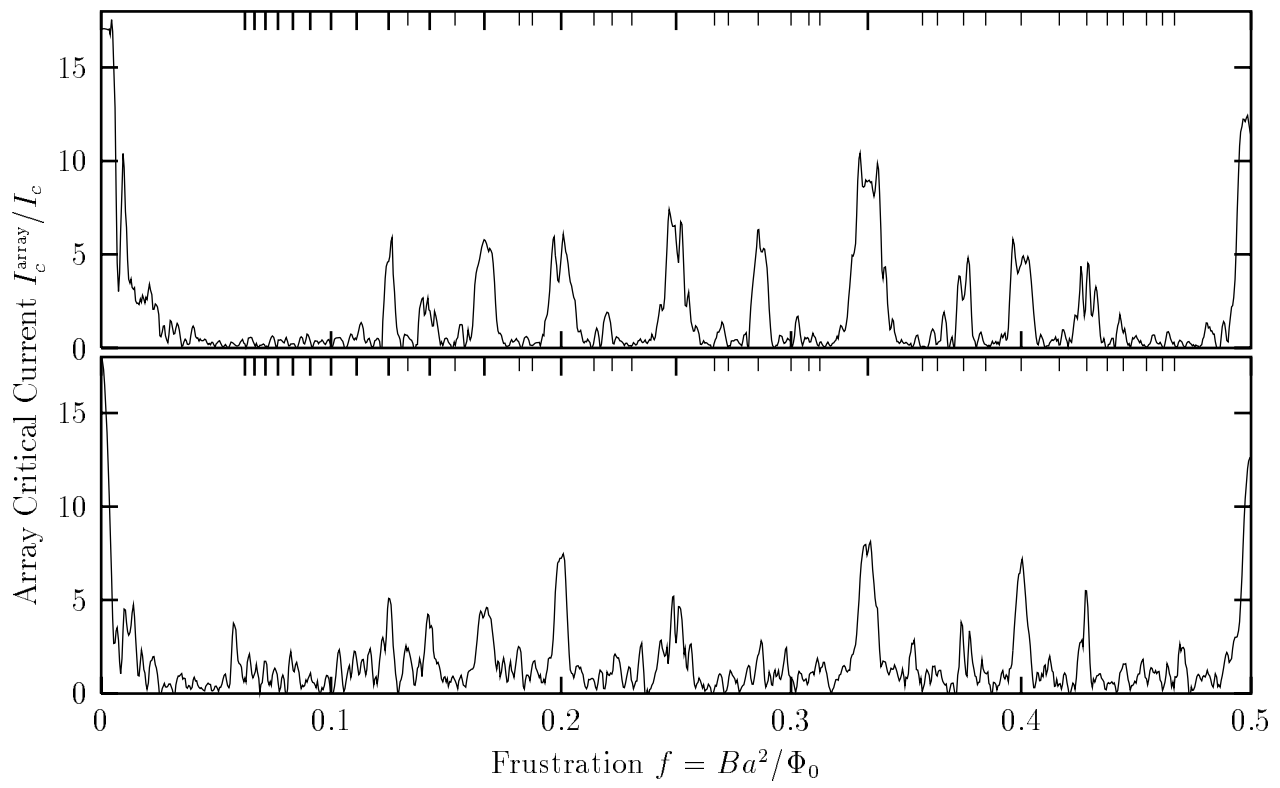


FIG. 3. Critical Currents of Josephson-Coupled Wire Arrays. J. Kent Harbaugh and D. Stroud.

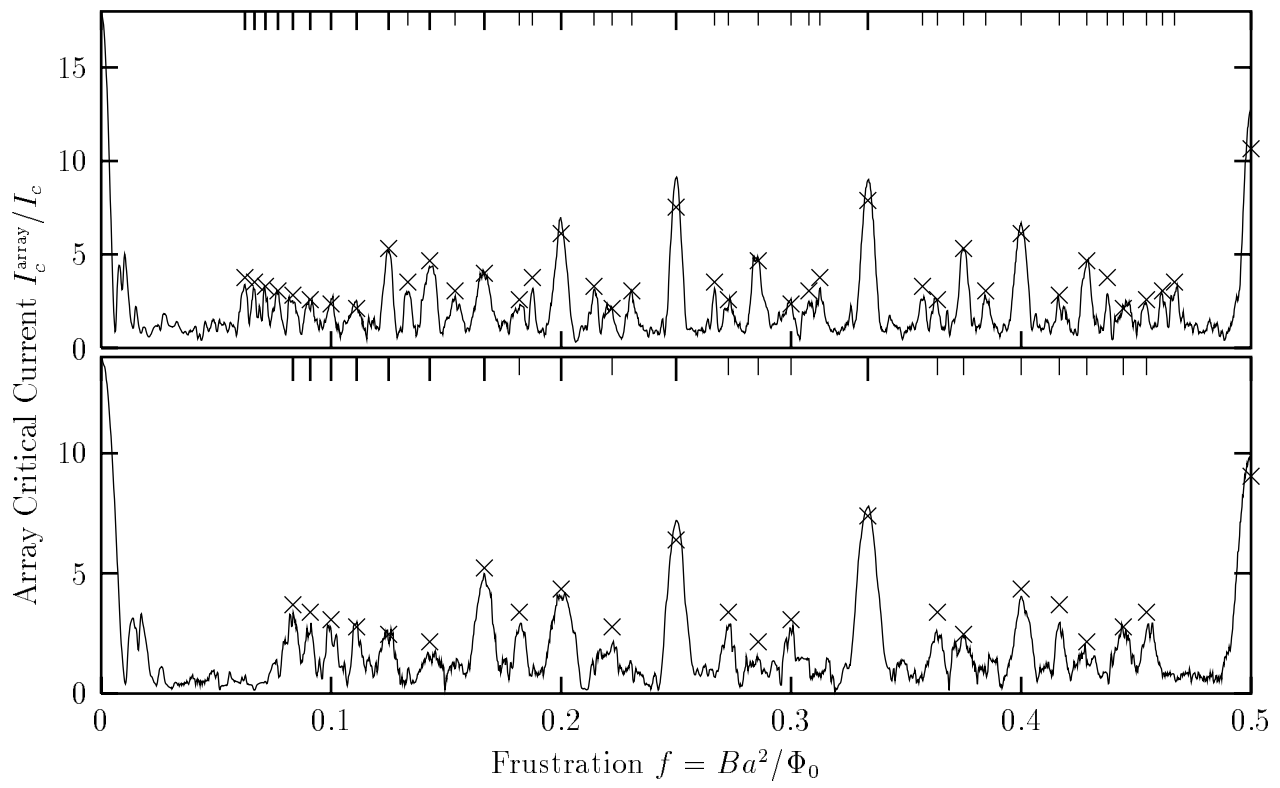


FIG. 4. Critical Currents of Josephson-Coupled Wire Arrays. J. Kent Harbaugh and D. Stroud.